

FRED-GMC: Filtering of Raw EPI Data for Gradient Map Calculations

F. Testud¹, O. Speck^{1,2}, J. Hennig¹, and M. Zaitsev¹

¹Dept. of Diagnostic Radiology, Medical Physics, University Hospital Freiburg, Freiburg, Germany, ²Dept. of Biomedical Magnetic Resonance, Otto-von-Guericke University, Magdeburg, Germany

Introduction: GRE EPI is sensitive to spatial and temporal changes of B_0 arising from susceptibility effects, temperature changes of the shims and motion of the object. This leads to time variant common image artefacts such as distortions and intensities losses.

Different correction techniques based on a field map or a PSF map acquired prior to a measurement yield parameters that determine the correction fields to be applied for subsequent measurements. However, temporal or spatial changes of B_0 during the scan are typically not taken into account. A possible remedy is the extraction of field gradients from the EPI raw data itself as was presented by Posse [1] for a GRE sequence and later by Deichmann et al. [2] and Chen et al. [3] for GRE EPI. In this work, we propose improvements to the method of Chen et al. [3] and compare them to the original method as well as to the method of Deichmann et al. [2].

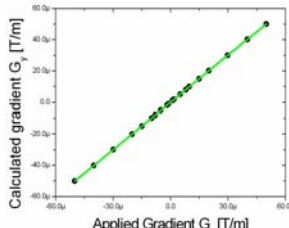


Fig. 1: Linear fit ($y = A + Bx$) for applied gradient G_y for a Gaussian filter function with $\sigma=2$

Method	B	S_B	A [$\mu\text{T}/\text{m}$]	S_A [$\mu\text{T}/\text{m}$]
Deichmann	0.9742	0.0062	-0.290	0.151
Chen	1.0056	0.0009	-0.010	0.021
Digital Delta function	1.0050	0.0041	-0.344	0.101
Gauss function, sigma = 2	1.0021	0.0003	0.050	0.007
Lorentz function, alpha = 0.55	1.0056	0.0017	-0.017	0.041

Table 1: Calculated gradients along phase encoding direction. B is the slope, S_B is the error of the slope, A the axis intercept and S_A is the error of the slope axis intercept.

We propose to replace the filter function by a Gaussian or Lorentzian function to account for the echo broadening under the influence of additional gradients. The additional parameters σ and α describe the width of the respective function. These parameters enable the contribution of additional lines to find the echo position. All the discussed methods do not have problems occurring from phase wrapping errors typical for phase map approaches.

Methods: All experiments were performed on a 3T system (Siemens Magnetom TRIO). A first experiment was performed with additional global gradients in x- and y-directions. The values were: ± 50 , ± 40 , ± 30 , ± 20 , ± 15 , ± 10 , ± 8 , ± 5 , ± 2 , ± 1 and 0 (applied only in one direction). The different filter functions and the methods [2] and [3] were implemented in Matlab. The phase map calculation from [2] was extended to the readout direction. After intensity masking of the gradient maps, the mean and the standard deviation was calculated and the background gradient was subtracted. The results were fitted to a linear function. The second experiment was performed with a GRE EPI with two echo times where gradients were applied simultaneously in both directions. The mean values of the absolute differences between applied and calculated gradients and the corresponding errors are calculated and displayed in Table 2.

Method	Mean of the difference for applied G_x gradients [$\mu\text{T}/\text{m}$]	Error of the difference for applied G_x gradients [$\mu\text{T}/\text{m}$]	Mean of the difference for applied G_y gradients [$\mu\text{T}/\text{m}$]	Error of the difference for applied G_y gradients [$\mu\text{T}/\text{m}$]
Deichmann	0.12	0.39	0.29	0.52
Chen	0.51	0.35	0.45	0.40
Digital Delta function	0.34	0.35	4.81	0.41
Gauss function, sigma = 2	0.18	0.36	0.05	0.43
Lorentz function, alpha = 0.55	0.17	0.36	0.03	0.43

Table 2: Differences and errors between the applied and the calculated gradients. The applied gradients were from $-15\mu\text{T}/\text{m}$ to $+15\mu\text{T}/\text{m}$ in steps of $5\mu\text{T}/\text{m}$ in x and y directions.

difference value than the methods from [3] or [2]. A field map was calculated from these gradients using a surface reconstruction algorithm [4] from surface normals using shapelets. The field map calculated with this algorithm is shown in Fig. 2 and compared to the field map calculated from two EPI images at different TE (Fig. 3). The two field maps differ in a constant due to the integration process. First in vivo measurements have been performed. Fig. 4 shows the gradient maps of a slice through the brain of a normal volunteer.

Conclusion and Outlook: The results show that our proposed filter functions are improving the accuracy of the results in comparison to the original method from [3] and sometimes also from [2]. These maps have yet to be transformed from the distorted EPI coordinate system to an undistorted coordinate system in order to become usable for distortion corrections. Filter approach developed here has reduced calculation overhead as compared to the method of Chen et al. [3], which makes it potentially applicable to the real-time prospective shim correction.

References:

- [1] S. Posse, MRM 25(1):12-29, May 1992
- [2] R. Deichmann et al., Neuroimage 15(1):120-135, June 2002,
- [3] N. Chen et al., Neuroimage 31(2):609-622, June 2006,
- [4] P. Kovesi, Technical report, School of Computer Science & Software Engineering, October 2003

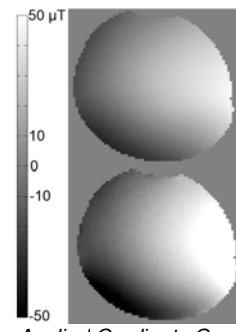


Fig. 2: Field map calculated with [4], Gaussian filter, $\sigma = 2$.

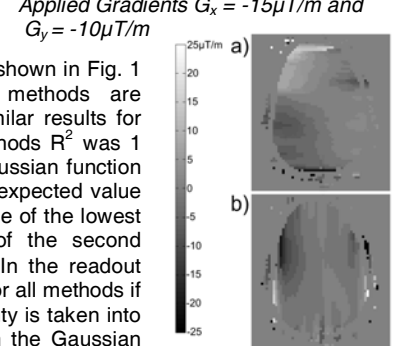


Fig. 3: Field map from two EPI images at different TE. $\Delta TE = 4\text{ms}$

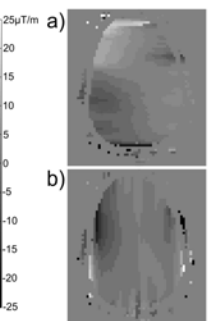


Fig. 4: Gradient maps Gaussian filter, $\sigma = 2$.
a) G_x Gradients
b) G_y Gradients